Structural and spectroscopical study of a 2,5-diphenyl-1,3,4-oxadiazole polymorph under compression

2006 J. Phys.: Condens. Matter 18 1459

(http://iopscience.iop.org/0953-8984/18/4/029)

INSTITUTE OF PHYSICS PUBLISHING JOURNAL OF PHYSICS: CONDENSED MATTER

J. Phys.: Condens. Matter **18** (2006) 1459–1472 doi:10.1088/0953-8984/18/4/029

Structural and spectroscopical study of a 2,5-diphenyl-1,3,4-oxadiazole polymorph under compression

O Franco[1,3], I Orgzall[2], W Regenstein[1] and B Schulz[1]

[1] University of Potsdam, Institute of Physics, Am Neuen Palais 10, D-14469 Potsdam, Germany
[2] Institute for Thin Film Technology and Microsensorics e.V., Kantstraße 55, D-14513 Teltow, Germany

E-mail: ofrancog@quim.ucm.es

Received 6 October 2005
Published 13 January 2006
Online at stacks.iop.org/JPhysCM/18/1459

Abstract

The x-ray pattern and the Raman and luminescence spectra of crystalline 2,5-diphenyl-1,3,4-oxadiazole in one of its polymorphic forms (DPO II) have been investigated under pressure up to 5 GPa. The behaviour of the lattice parameters under compression was determined and it was found that the Murnaghan equation of state provides a good description of the volume–pressure relationship of DPO II. The values for the bulk modulus and its pressure derivative are $K_0 = 8.6$ GPa and $K_0' = 7.2$. The analysis of the Raman spectrum under compression clearly shows the pressure-induced shift of the Raman modes to higher frequencies. The mode Grüneisen parameters for the lattice modes were determined. Additionally, it was found that the emission spectrum of DPO II moves to lower energies and that the luminescence intensity decreases when pressure is applied.

1. Introduction

Due to their promising characteristics as UV, blue and green emitters [1–3] and as electron-injection and hole-blocking layers [4–6], oxadiazole compounds have attracted great interest over the last years. In addition, they are able to build thin films, which is of crucial importance for applications in organic light emitting diodes (OLEDs) [7–9]. Oxadiazole derivates are used as chromophores, sensors, scintillators and material for OLEDs [10–12].

The characteristics of a material depend not only on its chemical formula but also on its molecular conformation and on its supramolecular arrangement. Therefore, in order to design new materials with optimized features, it is necessary to know more about the

[3] Author to whom any correspondence should be addressed. Present address: Departamento de Química Físca I, Facultad C Químicas, Universidad Complutense de Madrid, Ciudad Universitaria, 28040 Madrid, Spain.

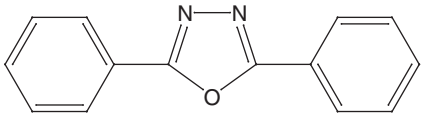

Figure 1. Chemical structure of DPO.

relationship between properties and structure. One way to modify the structure of a solid without introducing chemical changes in the materials is the application of high pressure. The controlled variation of the exerted pressure may serve to tune the properties of the material. Finally, to close the circle, the relation between structure and pressure (i.e. the compression mechanism of the substance) has to be determined. In view of the potential applications of the 1,3,4-oxadiazoles in LEDs and scintillators, their emission spectra at high pressure are of great interest. This study should be combined with the search for the structural change under compression.

The oxadiazole derivate we study in the present work is 2,5-diphenyl-1,3,4-oxadiazole (DPO, figure 1). Its crystal structure was firstly described by Kuznetsov *et al* [13]. A redetermination of this structure (DPO I) performed in our group gave the following results: monoclinic, space group $P2_1/c$, $a = 0.518\,85(6)$ nm, $b = 1.8078(2)$ nm, $c = 1.214\,35(14)$ nm, $\beta = 93.193(3)^\circ$ and $V = 1.1373(2)$ nm^3. Recently, we have found a second crystal structure (DPO II) which is non-centrosymmetric and shows non-linear optical activity [14]. The characteristic crystal parameters of DPO II are the following: monoclinic, space group Cc, $a = 2.4134(4)$ nm, $b = 2.4099(3)$ nm, $c = 1.2879(2)$ nm, $\beta = 110.048(3)^\circ$ and $V = 7.0363(17)$ nm^3. Calorimetric investigations combined with Raman studies showed that DPO I undergoes an irreversible phase transition into DPO II at 97 °C [14]. X-ray experiments under heating lend additional support to this result. Since two crystal structures of DPO exist in normal conditions and it is known that one transforms into the other under heating, it is necessary to clarify the structural behaviour of all polymorphs of DPO under compression.

The present study is a continuation of the work in references [15, 16], where the evolution of the crystal structure and of the emission spectrum of DPO I was investigated as a function of pressure. Here we aim to elucidate two points. First, the possibility of a pressure-induced phase transition of DPO II is examined. Second, the existence of similarities in the compression behaviour of DPO I and II is discussed. In particular, we consider the pressure-related evolution of volume and lattice parameters as well as Raman and luminescence spectra.

2. Experimental set-up

2.1. Sample preparation

2,5-di(phenyl)-1,3,4-oxadiazole was obtained following the usual procedure described in [14].

2.2. X-ray investigation

The structural investigations under compression were carried out using the multi-anvil high pressure device MAX-80 [17] in connection with the synchrotron radiation source of HASYLAB (Hamburg, Germany). The energy dispersive x-ray patterns were acquired with a Ge detector connected to a multi-channel analyser. The sample, in the form of powder, was introduced into an epoxy cube which serves as gasketing and pressure transmitting material. The pressure marker, NaCl, was also introduced into the cube. To prevent disturbances of

the diffractograms, the sample was not mixed with NaCl; they were placed in separate layers. The pressure within the cell was determined using the Decker equation for NaCl [18]. Slight pressure gradients of 0.1 GPa may be present in the sample.

The diffractograms were evaluated with the program Powder Cell 2.3 [19]. The theoretical pattern which results from the structure determination of a single crystal at ambient pressure was fitted to the experimental diffraction patterns. Powder Cell offers a specific resource to fit powder diffraction patterns. Through this option, the intensities of the different peaks are varied individually to neglect the influence of the powder technique. The precision of the determination of the lattice parameters from Powder Cell is estimated to 0.005 nm. From this approach only information about the lattice parameters, and not about crystal symmetry or atom positions, can be achieved. This method can only be applied if the crystal symmetry remains that of the ambient pressure structure. However, we checked that slight rotations and translations of the molecules, without modification of the crystal symmetry, preserve the structure of the powder x-ray pattern.

Thus, slight changes in the relative orientation of the molecules, such as those found in various oligo-(*para*-phenylenes) [20–23] or in anthracene [24–26] and some of its derivatives [27], cannot be excluded. Since such small modifications of the molecular arrangement are not taken into account in the model of Powder Cell, they will be carefully considered *a posteriori*. Additionally, in the fit procedure the rigid body approximation was used. This implies that the conformation of the molecule is assumed to remain constant.

2.3. Raman spectroscopy

The Raman measurements were performed using a He–Ne laser ($\lambda = 632.8$ nm) for excitation. The laser light was focused to a small spot of around 0.01 mm diameter. The laser output was reduced to less than 4 mW to avoid thermal heating effects of the sample. A triple Raman spectrometer system with a liquid nitrogen cooled CCD detector (T64000, Instruments S.A.) was used for recording the scattered light. An additional camera allowed the visual inspection of the sample and the precise localization of the laser spot on the sample. The resolution of the system was about 1 cm^{-1}. All spectra were calibrated using the spectral lines of Ne from a Pen Ray calibration lamp (LOT-Oriel).

For the achievement of high pressure in the spectroscopical studies (Raman and UV–vis spectroscopy) we employed a diamond anvil cell (DAC) [28]. We used a pre-indented Fe/Ni gasket. The sample was placed in the gasket hole (around 0.2 mm in diameter) together with a pressure marker and a pressure transmitting fluid. As pressure marker we used tiny ruby chips. The position of the R1 line of the fluorescence spectrum of ruby is calibrated as a function of pressure [29]. The error in the pressure determination was estimated to be up to 0.1 GPa. To achieve hydrostatic pressure the sample chamber was filled with Fluorinert F-77 (3M). This fluid guarantees hydrostatic conditions up to approximately 3.5 GPa and quasi-hydrostatic up to around 7 GPa. Fluorinert shows no remarkable absorption or luminescence signal in the spectral range which we have investigated.

2.4. Fluorescence spectroscopy

The absorption spectrum of the solution was acquired with a Lambda 19 spectrometer (Perkin Elmer). The emission measurements were performed using an Alphascan luminescence spectrometer (PTI). For the measurements of the crystals, the excitation and emission monochromators were coupled to the sample with quartz optic fibres. The fluorescence measurements at ambient pressure were carried out in a right-angle geometry whereas those

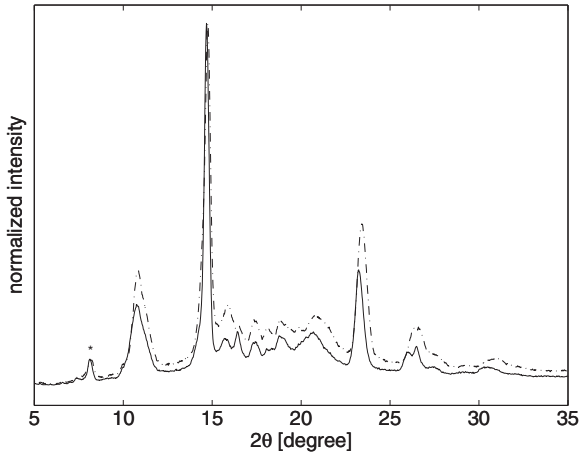

Figure 2. X-ray diffraction pattern of DPO II at 0 GPa before the compression (solid line) and at 0.2 GPa after the compression (dash–dotted line). The asterisk denotes an escape peak due to the detector material (Ge). Small influences of the gasketing cube may contribute to line broadening in the range from 16° to 22°. The energy dispersive diffractograms were converted to a 2θ-scale using the diffraction angle θ_E determined for NaCl in the closed pressure cell at ambient pressure and the wavelength corresponding to Cu Kα_1 radiation ($\lambda = 1.5406$ Å).

at high pressure (with the DAC) were performed in transmission set-up (in-line geometry), so that inner filter effects could not be avoided. To allow comparison, all measurements were made in steps of 0.5 nm and with a slit width of 2.5 nm.

3. Results and discussion

3.1. X-ray investigation at high pressure

Phase transitions and reversibility. The comparison of the x-ray patterns of DPO II at different pressures shows no significant differences in the shape of the patterns, just modifications attributable to an increased texture with pressure. Since no diffraction peaks appear or disappear, it is concluded that DPO II does not undergo phase transitions up to 4.9 GPa. Additionally, there are no discontinuities in the shift of the Raman lattice modes under compression, lending support to this conclusion (see section 3.2). A general decrease of the intensity with pressure is observed. This is principally due to the approximation of the anvils and hence the decrease of the radiation which passes through the sample and possibly also to a slight increase of the amorphous content. Such an enhancement of the amorphous component of the sample could also be concluded from the Raman investigation at high pressure and is also observed for other oxadiazole containing compounds [30].

After the compression run, the pressure was released and a diffraction pattern of the relaxed sample was acquired. Comparison of the patterns for the initial and the unloaded sample indicates that the compression is reversible (see figure 2). Moreover, no hysteresis was found. The pressure at the relaxation point was less than 0.2 GPa. A total relaxation could not be achieved due to the presence of stress in the sample, within the closed cell.

Lattice parameters at high pressure. The behaviour of the lattice parameters of DPO II under compression up to 4.9 GPa at room temperature is shown in figure 3. As is observed for other

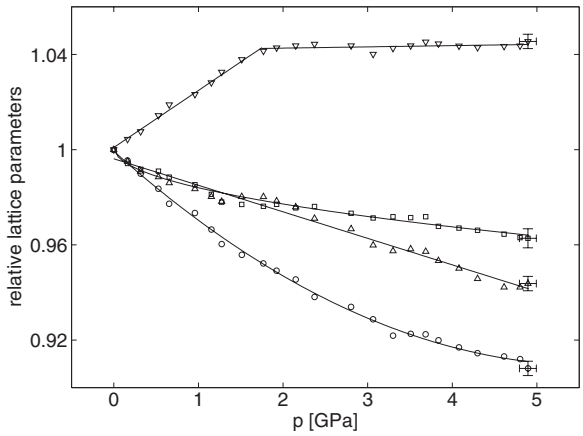

Figure 3. Relative lattice parameters of DPO II under compression (□ a/a_0, ○ b/b_0, △ c/c_0, ▽ β/β_0).

oxadiazole crystals (see [15, 31–34]), DPO II shows an anisotropic response to compression. This is a consequence of its crystal packing.

To facilitate the understanding of the compression of DPO II, a brief description of its molecular arrangement follows (for a complete crystal structure report see [14]). DPO II is built by nearly planar molecules arranged in layers parallel to the ab-plane (figure 4). The molecular planes are perpendicular to the layer plane. Different layers are connected through weak hydrogen bonds between a CH unit of the phenyl ring of one molecule and an N of the oxadiazole ring of another molecule (see [35–38] for a description of weak hydrogen bonds). Alternating stacks in zigzag arrangement build a layer. The molecules of adjacent stacks are perpendicular to each other. They interact through van der Waals forces between the phenyl rings. The molecular arrangement along a stack is reminiscent of the one encountered in DPO I (see [15, 14]). Parallel molecules are placed in such a way that the oxadiazole unit of a molecule is sandwiched between the phenyl rings of the adjacent molecules, leading to the formation of π-complexes. In the stacks of DPO II, however, every third molecule is oriented in the opposite direction (referring to the oxadiazole ring) in relation to its neighbours, whereas in DPO I the molecules of a stack share the same orientation.

Rotations or translations of the molecules of a stack would lead to the destabilization and break-up of the π-complexes and hence to important changes in the crystal packing, that is, to a phase transition. Since we have probed that no phase transitions appear in the pressure range up to 4.9 GPa, we propose that the π-complexes and the stack arrangement are maintained during the compression. The only possible movements in DPO II crystals are translations of the entire stacks and hence also of the layers as a whole, as well as the parallel approximation of the molecules within a stack.

The arrangement of the molecules in stacks within a layer is such that the a- and b-axes of the unit cell are expected to behave in the same way. The π–π interactions between the molecules of the two sets of stacks are oriented along a and b, respectively. Additionally, the weak van der Waals forces which act between the stacks are also equal in both directions. However, the non-maintenance of β under compression disturbs the expected similarity. β increases up to 1.8 GPa and at higher pressure remains nearly constant. The increment in the monoclinic angle is expected to produce the approximation of the stacks and to reduce the distance between those molecules (within a stack) which are perpendicular to a. This would

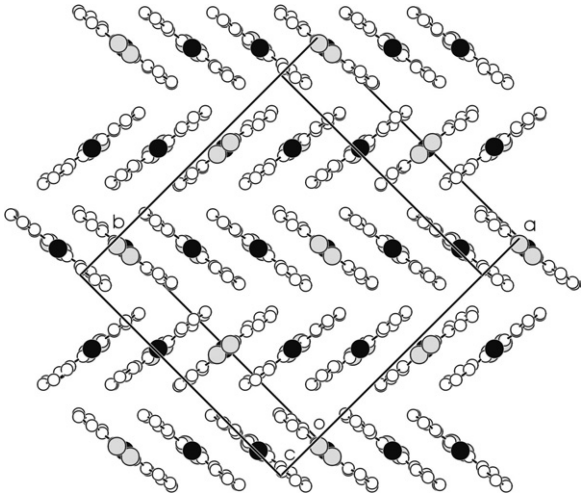

Figure 4. Molecular arrangement of DPO II. View of a layer.

explain why the decrease of the length of a up to approximately 1.5 GPa is not as large as the one experienced by b. Beyond this value of pressure, β remains nearly constant and a decreases only slightly. The molecules perpendicular to a may be so close together that the electrostatic repulsion between the components of the π-complexes may prevent the compression of a as well as any further increase of β. However, though consistent with the measurements, this hypothesis cannot be proven with the present data; single-crystal high pressure diffraction or molecular modelling is necessary.

The interaction of molecules of different layers in DPO II (the layers are perpendicular to c) is very similar to that found for adjacent stacks along the c-axis of DPO I. In both cases there are weak hydrogen bonds between the CH groups of the phenyl rings and the N atoms of the oxadiazole unit with very close characteristic parameters [14, 15, 33]. Therefore, a similar behaviour under compression of the c-axes of DPO I and II is expected. It is significant to note that the linear compressibility of c of DPO I after 1.3 GPa (0.010 GPa^{-1}) is nearly identical to that found for c of DPO II in the whole pressure range (0.011 GPa^{-1}).

Equation of state. From the lattice parameters at every pressure step the volume of the unit cell is directly obtained. The isothermal volume as a function of pressure is shown in figure 5 for DPO II up to 4.9 GPa. The experimental data are well described by the Murnaghan equation of state (MEOS) [39]:

$$p = \frac{K_0}{K_0'}\left[\left(\frac{V_0}{V}\right)^{K_0'} - 1\right] \tag{1}$$

with $K_0 = 8.6$ GPa and $K_0' = 7.2$. The small value of the bulk modulus (K_0) indicates a large compressibility of DPO II in the investigated interval. For comparison, we include in figure 5 the volume decrease of other oxadiazole crystals up to approximately 5 GPa: DPO I, the two-ring containing molecule 4-(5-methyl-1,3,4-oxadiazole-2yl-)-N, N'-dimethyl-phenylamine (MODPA) and 2,5-di-(4-aminophenyl)-1,3,4-oxadiazole (DAPO I) from [15, 32]. The decrease of the normalized volume of these oxadiazole crystals is quite similar and moreover it is in the same range as that found for similar aromatic compounds such as biphenyl, *para*-terphenyl and further oligo-(*para*-phenylenes) [23, 40]. The weakness of the

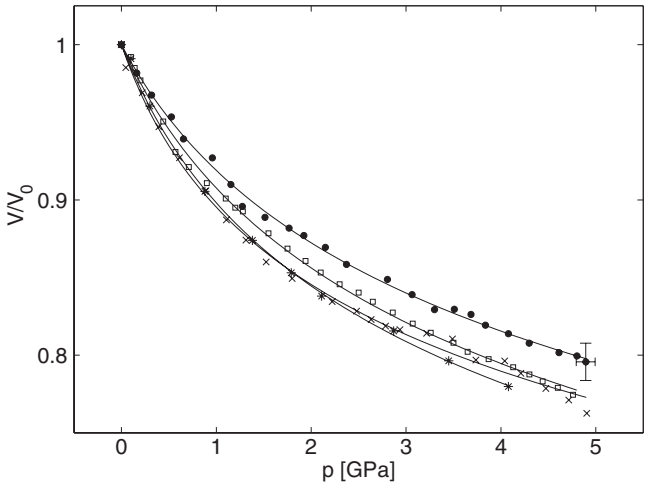

Figure 5. From top to bottom: relative volume of DPO II (•), DPO I (□), DAPO I (×) and MODPA (∗) under compression. The lines are the corresponding MEOSs.

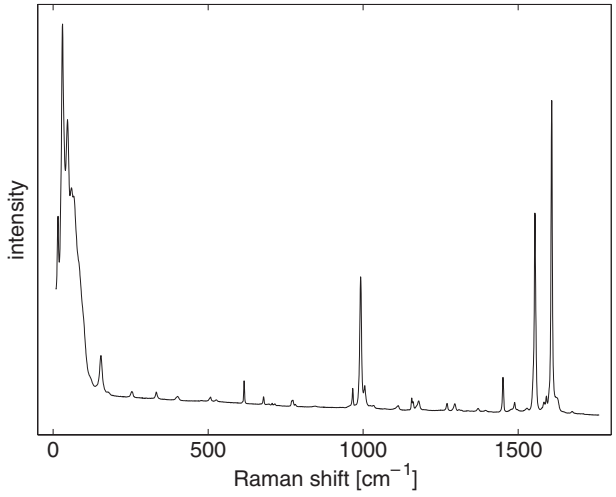

Figure 6. Raman spectrum of DPO II at ambient conditions.

intermolecular interactions in these organic crystals, compared with ionic, covalent or metallic crystals, causes their softness.

3.2. Raman spectra under compression

Figure 6 shows the Raman spectrum of DPO II at ambient pressure in the fingerprint region below 2000 cm^{-1}. There are three regions with strong and very strong bands: the region of the lattice vibrations which goes up to around 200 cm^{-1} and two regions of internal modes, one around 1000 cm^{-1} and the other between 1450 and 1650 cm^{-1}, dominated by the ring-vibrations of the phenyl and oxadiazole groups. A detailed description of the Raman spectrum of DPO II and its comparison with that of DPO I was reported in [14]. Therefore, it will not be discussed here.

Table 1. Frequencies at ambient pressure, their pressure derivatives at ambient pressure and the mode Grüneisen parameters (γ_i) of selected Raman modes of DPO II.

ν_i (cm^{-1})	$d\nu_i/dp$ (cm^{-1} GPa^{-1})	γ_i
16	5.4	2.91
32	5.0	1.34
31	13.3	3.69
45	14.1	2.66
59	16.7	2.45
70	9.1	1.12
95	22.6	2.05
103	22.1	1.85
155	20.7	1.15
192	12.0	0.54
967	1.7	0.02
992	3.9	0.03
1005	3.3	0.03
1451	2.8	0.02
1488	3.0	0.02
1554	5.0	0.03
1584	6.6	0.04
1591	4.2	0.02
1608	4.7	0.03
1626	9.3	0.05

When a substance undergoes phase transitions, major changes in its vibrational spectrum occur [41]. This is a consequence of the differences between the space groups and hence between the selection rules of the two phases. The comparison of the Raman spectra of a crystal of DPO II at pressures up to 5.2 GPa shows no major modifications in its vibrational spectrum. Thus, the high pressure Raman investigation confirms the absence of pressure-induced phase transitions in DPO II, concluded from the x-ray study.

DPO II shows a continuous shift of the vibrational modes to higher frequencies and a general intensity decrease and background increase under compression. The frequency shift is fully reversible and free of hysteresis, while the other effects, the intensity decrease and background increase, show just a slight irreversibility. Figure 7 shows the frequency shift of selected Raman lines of DPO II. It is worth noting that the modes show a slight non-linear shift in the very low pressure region. The pressure coefficients $d\nu_i/dp$ which describe the shift are summarized in table 1. The increase in the vibrational frequencies can be explained by the anharmonicity of the vibrations [41]. When the crystal is compressed, the inter-atomic distances decrease, resulting in an increase in the effective force constants and therefore in the vibrational frequencies. The shifts of the lattice modes are mostly one order of magnitude larger than those of the internal modes. This means that during the compression the molecules as a whole approximate more than the atoms within the molecules, e.g. the shortening of the lattice parameters is more intense than that of the molecular bonds. The second effect, the intensity decrease with compression, results from a slight increase of the amorphous portion under compression. It seems that at high pressure the number of defects in the crystal structure increases. X-ray investigations under compression corroborate this statement.

From the values of $d\nu_i/dp$ and the MEOS, the dependence of the Raman frequencies on volume can be easily calculated. Thus, the mode Grüneisen parameters for the lattice modes were determined as follows (see table 1):

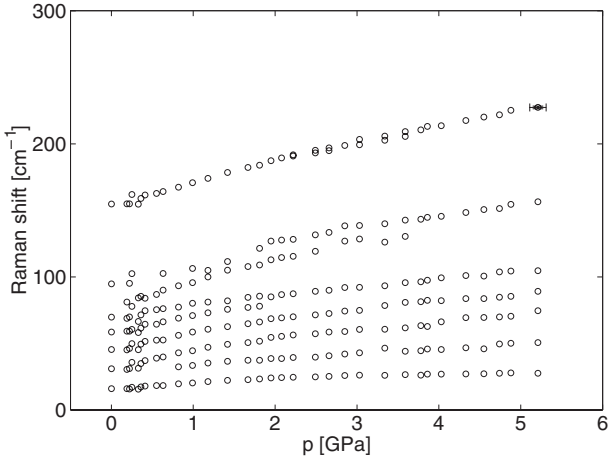

(a) Region of the lattice vibrations.

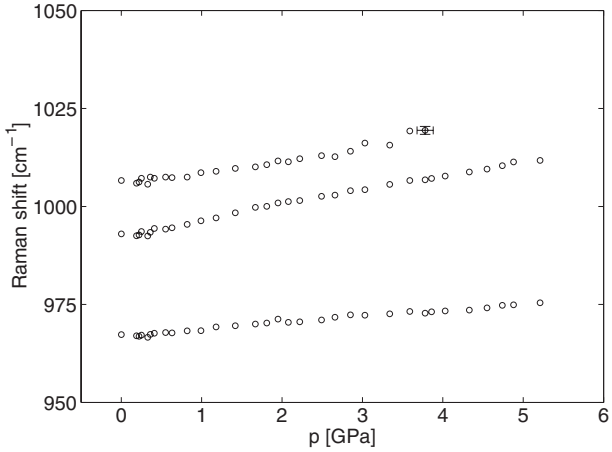

(b) Region around 1000 cm^{-1}.

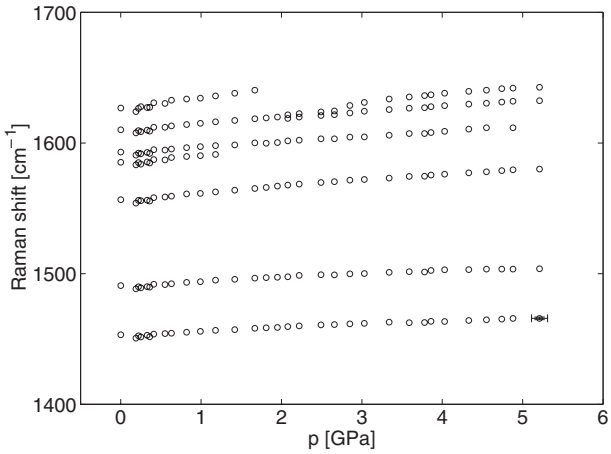

(c) Region between 1400 and 1700 cm^{-1}.

Figure 7. Shift of the Raman lines of DPO II as a function of pressure.

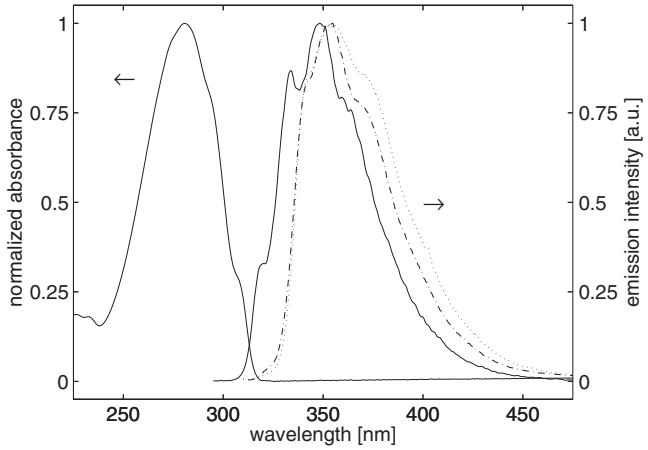

Figure 8. Left: absorption spectra of DPO in ethanol. Right: emission spectra of DPO in ethanol (solid curve), of DPO I crystals (dash–dotted curve), and of DPO II crystals (dotted curve).

$$\gamma_i = -\left.\frac{\mathrm{d}\ln\nu_i}{\mathrm{d}\ln V}\right|_{V_0} = -\left.\frac{K_0}{\nu_i}\frac{\mathrm{d}\nu_i}{\mathrm{d}p}\right|_{p=0}. \tag{2}$$

Knowing the mode Grüneisen parameters γ_i, an estimation of the Debye–Grüneisen parameter should be possible (for instance as a mean value weighted by the real spectrum). Thus, although the Raman modes only constitute one part of the total vibrational modes (they should be completed with the infrared modes and the acoustic lattice modes), the relation between their frequencies and pressure combined with the MEOS represents an important contribution to the construction of a thermodynamic equation of state for the system in the frame of an extended Debye model [42]. It should be noted that the mode Grüneisen parameters determined for DPO II are in the same range as those calculated for DPO I and other oxadiazole crystals [33].

3.3. Luminescence spectra at ambient pressure

The absorption spectrum of a dilute solution of DPO in ethanol ($c = 10^{-5}$ mol l^{-1}) shows two bands in the UV range, located at 230 and 280 nm (see figure 8), in agreement with the results of Popova *et al* [43] and Feygelman *et al* [44]. We coincide with these authors in the assignment of the long-wave band to a $\pi\pi^*$ transition delocalized along the molecule and have proposed that the small short-wave band is associated with an $n\pi^*$ transition localized at the hetero-atoms of the oxadiazole ring [33]. The excitation at the $\pi\pi^*$ absorption band induces an intense emission with vibrational structure and maximum at 349 nm (figure 8). The overlap between absorption and fluorescence induces an inner filter effect which distorts the shape of the fluorescence curve at short wavelengths.

The fluorescence of the DPO I and II crystals corresponds well with that of the solution, but it is slightly red shifted with respect to the latter (figure 8). The emission spectra of DPO in crystalline form do not show any additional bands with respect to the spectrum of the solution. Therefore, the individual molecule determines to a large extent the optical properties of the crystal. The fluorescence of both DPO I and II shows a peak at 353 nm and a shoulder at 374 nm. In spite of having different crystal structures, the DPO polymorphs share the same

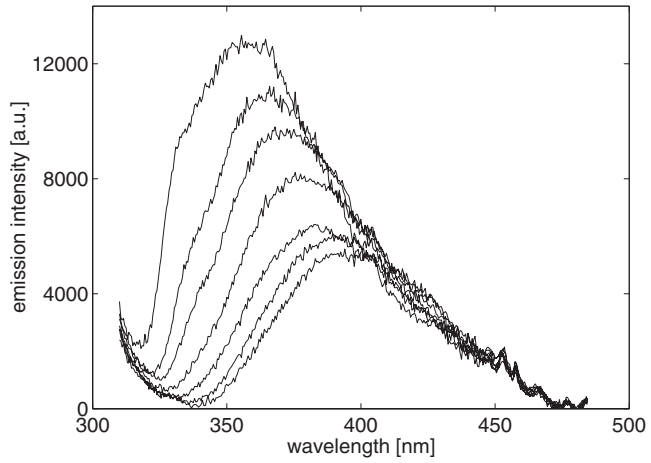

Figure 9. Emission spectra of DPO II crystals at different pressure values: from top to bottom, 0.6, 1.4, 2.0, 3.0, 3.6, 5.0 and 5.4 GPa.

fluorescence spectra, with only small divergences in the relative intensities of the peak and the shoulder. This coincidence is caused by the similarity both in the molecular conformations in DPO I and II and in their inter-molecular π–π interactions along a stack [14, 33].

One of the reasons for the red shift is the presence of partial conjugation of the π electron system in the nearly planar molecules of the crystals, which contrasts with the lack of conjugation in the non-planar dissolved molecules (their rings can rotate freely around the molecular axis). The appearance of partial conjugation induces the increase of the bandwidth of the ground and excited states, which in turn leads to a lowering of the transition energy [20, 22, 45]. Besides, the stack-like arrangement of the crystals favours a certain overlap of the wavefunctions of neighbouring molecules in the stack. Such overlap, which corresponds to the π–π interaction within the stacks, implies a further broadening of the energy levels and therefore a decrease of the transition energy [20, 22, 45, 46].

3.4. Luminescence spectra under compression

The compression of the crystal induces a red shift of its emission spectrum and a decrease of the fluorescence intensity (figures 9 and 10). The short wavelength edge of the emission band loses its sharpness progressively with pressure due to the decrease of the inner filter effect (as preliminary absorption experiments—not shown here—confirm). However, the distortion of the band's shape at low values of pressure is only perceptible in the foot of the short-wave edge and does therefore not affect the width of the curves at 70% of its maximum value. Taking into account this width, we conclude that the emission band does not experience a broadening under compression. When pressure is released, the fluorescence spectrum returns to its initial state (within the experimental limits).

Again, there may be two causes for the decrease of the transition energy under compression: a possible increase of the partial conjugation of the π system along the molecule and the intensification of the interactions between molecules. An increase of the partial conjugation may result from the planarization of the molecules and/or from the shortening of the inter-ring bonds under compression. In the case of DPO II, a possible planarization of the molecules under compression should be negligible since they are already nearly perfectly planar at ambient pressure (the mean deviation from planarity is 6°). Puschnig *et al* have calculated

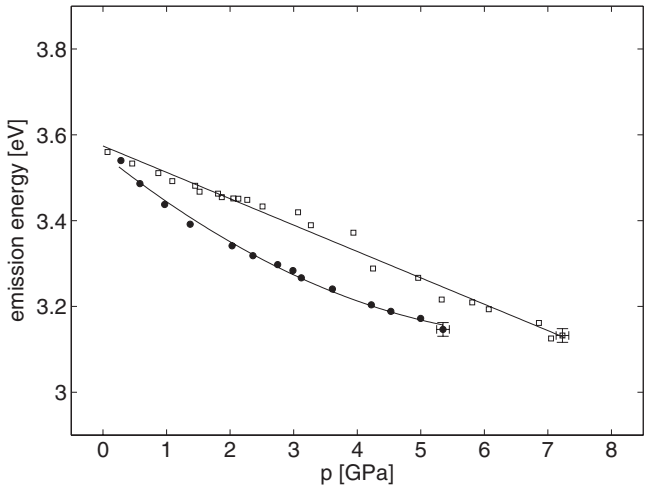

Figure 10. Energy shift of the emission maximum of DPO I (□) and DPO II (•) crystals as a function of pressure. The lines correspond to the fits described in the text.

changes of the inter-ring bond lengths for *para*-terphenyl of 0.001 nm up to 5 GPa [22]. The similarity between *para*-terphenyl and DPO allows us to expect comparable inter-ring shortenings in our case. On the other hand, comparison of the emission bands of DPO I and II at ambient pressure indicates that differences of the inter-ring bond lengths by 0.001 nm do not modify the spectra (for the molecular conformation at ambient pressure of DPO I and II see [13, 14]). Thus, possible changes on the molecular conformation induced by pressure scarcely influence the emission spectrum of DPO II in the present pressure range. The decisive factor which induces the red shift is therefore the increased intensity of the inter-molecular interactions within the crystal, in agreement with the calculations of Puschnig *et al* for the oligo-(*para*-phenylenes) [21, 22]. The electronic transition responsible for the fluorescence is a $\pi\pi^*$ transition. Consequently, it is expected to be very sensitive to the intensification of the π–π interactions along the stacks.

For comparison we added to figure 10 the energy shift of the emission of DPO I, from [16]. The energy shifts of DPO I and II are in the same range, due to the resemblance of their molecular geometry and due to the presence of similar molecular stacks in both crystals. The energy shift of the luminescence can be described by the relations $E_{\mathrm{lum}}/\mathrm{eV} = 3.57 - 0.061\,p/\mathrm{GPa}$ for DPO I and $E_{\mathrm{lum}}/\mathrm{eV} = 3.55 - 0.118\,p/\mathrm{GPa} + 0.008\,p^2/\mathrm{GPa}^2$ for DPO II in the ranges up to 7.2 and 5.4 GPa, respectively. These shifts are slightly larger than, though of the same order of magnitude as, those calculated for *para*-terphenyl (linear reduction of the band gap with a pressure coefficient of -0.04 eV GPa^{-1}) [22]. The reason for the relatively large red shift of DPO I and II is the strong way in which their π-orbitals are influenced by pressure. This results from the particular stack-like supramolecular structure of the DPO polymorphs.

Figure 9 also shows a decrease of the intensity of the emission spectra with pressure. This effect may be due to several factors. One factor is the diminution of the transition energy which favours the thermal deactivation of the excited state. Two further factors connected with the presence of quenching sites are relevant. Firstly, the number of quenching sites due to defects in the crystal increases under compression, as the high pressure x-ray and Raman experiments indicate. Secondly, as a result of the enhanced orbital overlap, the electronic mobility increases, which in turn leads to a higher probability of occupation of the quenching sites.

4. Conclusions

The present study is motivated by previous work on DPO [14–16], where it was found that two polymorphic forms (DPO I and II) exist at ambient pressure and that an irreversible phase transition of DPO I into II takes place under heating. Furthermore, the behaviour of both the crystal structure and the luminescence spectrum of DPO I under compression was discussed. Two important questions arising from these earlier studies could be answered here: does the compression of DPO II cause phase transitions, and is the pressure dependence of the Raman and emission spectra of DPO II analogous to that of DPO I?

Our present x-ray and Raman studies at high pressure demonstrate that DPO II does not undergo pressure-induced phase transitions. Moreover, the high pressure x-ray investigation shows that the volume decrease of DPO II is similar to that of DPO I and other oxadiazole crystals. The small value of K_0 confirms the expected softness of DPO II. Its particular crystal structure determines the strongly anisotropic compression of DPO II. Due to differences in the molecular arrangement of the polymorphs of DPO, a direct comparison is only possible with respect to their c-axes, for which nearly identical linear compressibilities were determined.

It was observed that the Raman lines move to higher frequencies with pressure. Combining this finding with the MEOS, we calculated the mode Grüneisen parameter for the external Raman modes of DPO II. They are in the same range as those of DPO I.

The emission spectra of DPO I and II are red shifted in relation to the solution spectrum. This red shift is due to the appearance of a partial conjugation in the molecules and to the increase of the inter-molecular interactions in the crystals compared to the solution. The red shift effect becomes more pronounced when the crystals are compressed. We propose that the decisive factor for the pressure-induced red shifts is the enlargement of the inter-molecular interactions within the crystals as a result of the volume decrease. It is worth noting that the luminescence spectra of DPO I and II at ambient pressure are identical and their shifts with pressure are in the same range.

Another effect which occurs when the crystal is compressed is the decay of its emission intensity. This phenomenon is due to the increased radiationless deactivation of the excited state and to the increment of the quenching sites during the compression. In relation to this, it should be mentioned that our present x-ray and Raman investigations confirmed the increase of defects in the crystal structure with pressure.

Acknowledgments

We thank Ch Lathe and the GeoForschungsZentrum Potsdam for the possibility of using the MAX-80 equipment. We acknowledge as well the support of the Deutsche Forschungsgemeinschaft through grants No Or 78/3-2 and SCHU 842/12-3.

References

[1] Hwang S W and Chen Y 2002 *Macromolecules* **35** 5438–43
[2] Kaminorz Y, Schulz B and Brehmer L 2000 *Synth. Met.* **111/112** 75–8
[3] Huang W, Meng H, Yu W L, Gao J and Heeger A J 1998 *Adv. Mater.* **10** 593–6
[4] Ma W, Iyer P K, Gong X, Liu B, Moses D, Bazan G C and Heeger A J 2005 *Adv. Mater.* **17** 274–7
[5] Zeng L, Yang M, Wu P, Ye H and Liu X 2004 *Synth. Met.* **144** 259–63
[6] Wang C, Jung G Y, Batsanov A S, Bryce M R and Petty M C 2002 *J. Mater. Chem.* **12** 173–80
[7] Xu C, Kaminorz Y, Reiche J, Schulz B and Brehmer L 2003 *Synth. Met.* **137** 963–4
[8] Franco O, Katholy S, Morawetz K, Reiche J, Freydank A, Brehmer L and de Saja J A 2002 *Colloids Surf.* A **198** 119–26

[9] Kaminorz Y, Xu C, Schulz B, Stiller B, Reiche J, Regenstein W and Brehmer L 2002 *Synth. Met.* **127** 217–20
[10] Zhou G, Cheng Y, Wang L, Jing X and Wang F 2005 *Macromolecules* **38** 2148–53
[11] Heo J S, Park N H, Ryo J H and Suh K D 2005 *Adv. Mater.* **17** 822–6
[12] Ma D, Liang F, Wang L, Lee S T and Huang L S 2002 *Chem. Phys. Lett.* **358** 24–8
[13] Kuznetsov V P, Patsenker L D, Lokshin A I and Tolmachev A V 1998 *Crystallogr. Rep.* **43** 430–8
[14] Franco O, Orgzall I, Reck G and Schulz B 2003 *J. Mol. Struct.* **649** 219–30
[15] Franco O, Reck G, Orgzall I and Schulz B 2002 *J. Phys. Chem. Solids* **63** 1805–13
[16] Franco O, Regenstein W, Orgzall I and Schulz B 2002 *High Pressure Res.* **22** 131–4
[17] Shimomura O, Yamaoka S, Yagi T, Wakatsuki M, Tsuji K, Kawamura H, Hamaya N, Fukunaga O, Aoki K and Akimoto S 1985 Multi-anvli type x-ray system for synchrotron radiation *Solid State Physics under Pressure* ed S Minomura (Dordrecht: Reidel)
[18] Decker D L 1971 *J. Appl. Phys.* **42** 3239–44
[19] Kraus W and Nolze G 1999 *PowderCell 2.3* (Berlin: BAM)
[20] Puschnig P, Ambrosch-Draxl C, Heimel G, Zojer E, Resel R, Leising G, Kriechbaum M and Graupner W 2001 *Synth. Met.* **116** 327–31
[21] Puschnig P, Heimel G, Weinmeier K, Resel R and Ambrosch-Draxl C 2002 *High Pressure Res.* **22** 105–9
[22] Puschnig P, Hummer K and Ambrosch-Draxl C 2003 *Phys. Rev.* B **67** 235321–7
[23] Heimel G, Puschnig P, Oehzelt M, Hummer K, Koppelhuber-Bitschnau B, Porsch F, Ambrosch-Draxl C and Resel R 2003 *J. Phys.: Condens. Matter* **15** 3375–89
[24] Oehzelt M, Resel R and Nakayama A 2002 *Phys. Rev.* B **66** 174104–5
[25] Oehzelt M, Weinmeier K, Heimel G, Puschnig P, Resel R, Ambrsch-Draxl C, Porsch F and Nakayama A 2002 *High Pressure Res.* **22** 343–7
[26] Oehzelt M, Heimel G, Resel R, Puschnig P, Hummer K, Ambrsch-Draxl C, Takemura K and Nakayama A 2003 *J. Chem. Phys.* **119** 1078–84
[27] Brillante A, Della Valle R G, Polizzi C and Syassen K 1999 *Physica* B **265** 199–202
[28] Jayaraman A 1983 *Rev. Mod. Phys.* **55** 65–108
[29] Forman R A, Piermarini G J, Barnett J S and Block S 1972 *Science* **176** 284–5
[30] Luo J F, Han Y H, Tang B C, Gao C X, li M and Zou G T 2005 *J. Phys. D: Appl. Phys.* **38** 1132–5
[31] Orgzall I, Lorenz B, Mikat J, Reck G, Knochenhauer G and Schulz B 1999 *J. Phys. Chem. Solids* **60** 1949–65
[32] Franco O, Orgzall I, Reck G, Stockhause S and Schulz B 2005 *J. Phys. Chem. Solids* **66** 994–1003
[33] Franco O 2002 Structural and spectroscopical study of crystals of 1,3,4-oxadiazole derivatives at high pressure *PhD Thesis* Universität Potsdam
[34] Orgzall I, Franco O, Reck G and Schulz B 2005 *J. Mol. Struct.* **749** 144–54
[35] Meléndez R E 1998 Hydrogen-bonded ribbons, tapes and sheets as motifs for crystal engineering *Design of Organic Solids* (*Springer Topics in Current Chemistry* vol 198) ed E Weber (Berlin: Springer)
[36] Desiraju G R 2002 *Acc. Chem. Res.* **35** 565–73
[37] Steiner T 1997 *Chem. Commun.* **8** 727–34
[38] Steiner T and Desiraju G R 1998 *Chem. Commun.* **8** 891–2
[39] Poirier J P 1991 *Introduction to the Physics of the Earth's Interior* (Cambridge: Cambridge University Press)
[40] Beggerow G 1980 Eigenschaften der materie bei hohen drücken *Zahlenwerte und Funktionen aus Naturwissenschaften und Technik* (*Makroskopische und Technische Eigenschaften der Materie. Gruppe IV. Landolt-Börnstein. Neue Serie*) (Berlin: Springer)
[41] Ferraro J R 1984 *Vibrational Spectroscopy at High External Pressures* (Orlando, FL: Academic)
[42] Kieffer S W 1979 *Rev. Geophys. Space Phys.* **17** 1–19
[43] Popova N A, Yushko E G, Krasovitskii B M, Minkin V I, Lyubarskaya A E and Goldberg M L 1983 *Khim. Geterotsiklich. Soed.* **1** 26–32
[44] Feygelman V M, Walker J K, Katrizky A R and Dega-Szafran Z 1989 *Chem. Scr.* **29** 241–3
[45] Puschnig P and Ambrosch-Draxl C 1999 *Phys. Rev.* B **60** 7891–8
[46] Hummer K, Puschnig P and Ambrosch-Draxl C 2003 *Phys. Rev.* B **67** 184105–7